

# GLOBAL JOURNAL OF ENGINEERING SCIENCE AND RESEARCHES

## PERFORMANCE IMPROVEMENT OF LINEAR MOTOR PARAMETER IDENTIFICATION VIA OPERATION SPACE DIVISION

Gyu-Sik Kim\*<sup>1</sup> and Sung-Ha Yun<sup>2</sup>

\*<sup>1,2</sup> Department of Electrical Engineering, The University of Seoul, Seoul, Korea

### ABSTRACT

A conventional reciprocating compressor uses a crank mechanism in order to change the rotational motion of a motor into linear motion. Accordingly, a reciprocating compressor can be operated safely by virtue of the crank mechanism, even though it makes the reciprocating compressor less efficient. However, the moving parts of a linear compressor are not constrained. Thus, the implementation of a closed-loop control system is necessary for the accurate control of piston position. In this paper, a sensorless linear compressor control system with motor parameter identification is implemented. Various motor parameter identification algorithms are evaluated to demonstrate the practical significance of our results.

**Keywords:** *linear motion, linear compressor, sensorless control, piston position, motor parameter identification*

### I. INTRODUCTION

A small linear compressor which operates at 50Hz was designed for the European market which could serve a variety of small and portable coolers for specialty uses, including recreational or medical cooling [1]. The piston positioning accuracy and the efficiency of the sensorless linear compressor system with the linear pulse motor were examined using analytical and experimental approaches [2]. But, the motor parameters were not identified fully. A dual stroke and phase control system was proposed for linear compressors of a split-stirling cryocooler [3]. A linear compressor was developed for 680 liter household refrigerator [4]. It reduced the energy consumption of a refrigerator by 47% compared with a reciprocating compressor. In [5], they showed that LGE created the innovative linear compressor, which has much higher efficiency in the small cooling capacity. The refrigerator with this linear compressor shows that the power consumption reduction by 25% can be achieved, as compared with the reciprocating compressors.

The results of an investigation on the system dynamics and the controller design of a linear compressor for stroke and frequency adjustment were presented [6]. A system dynamics model was derived and identified experimentally. A control system was designed based on the system dynamics model. The control system used a PDF (Pseudo-Derivative Feedback) algorithm. A linear compressor operated directly by commercial AC electricity was developed in order to reduce the cost by eliminating the expensive controller and to enhance the compatibility with various types of refrigerators [7]. Parameters of the linear compressor were adjusted to get robust performances against the fluctuations of load and outlet voltage. Results of experiments showed the start linear compressor maintained high efficiency and low noise as well as excellent reliabilities even in severe conditions of household refrigerators. The simulation and experimental investigations on the static and dynamic characteristics of a moving magnet linear motor and a moving magnet linear compressor were presented [8]. Also, the force and equilibrium characteristics of the linear motor have been predicted and verified by detailed static experimental analyses.

The performance of linear compressors using a pulse width modulation inverter is investigated, with emphasis on the efficiency and power factor along with variations of both mechanical and electrical resonant frequencies [9]. In [9], the strategy for improving the efficiency of the linear compressor was suggested by controlling the average value of the product of the piston stroke and motor current to 0. The mathematic model of the self-sensor was established by analyzing the moving magnet linear motor of linear compressor, and the measurement method of piston stroke was achieved [10]. In [10], the piston stroke can be calculated by measuring the voltage and current of the linear motor coil.

The closed-loop sensorless stroke control system for a linear compressor has been designed. The motor parameters are identified as functions of piston position and motor current. Then, they are stored in a read-only memory (ROM) table and used later for accurate estimation of piston position [11].

In this study, we improved the results in [11]. We divided the linear compressor operation space into several parts. Hence, even though the first-order approximation of identified motor parameters, the errors might be decreased.

## II. IMPLEMENTATION OF SENSORLESS LINEAR COMPRESSOR DRIVES

The mechanical structure of the linear compressor studied in this research is shown in Fig. 1. The equivalent electrical circuit of a linear motor in a linear compressor can be modeled and expressed as the linear differential Eq. (1). The thrust force is expressed in Eq. (2).

$$\alpha \frac{dx(t)}{dt} + L_e \frac{di(t)}{dt} + R_e i(t) = V(t) \tag{1}$$

$$F_e(t) = \alpha i(t) \tag{2}$$

Figure:

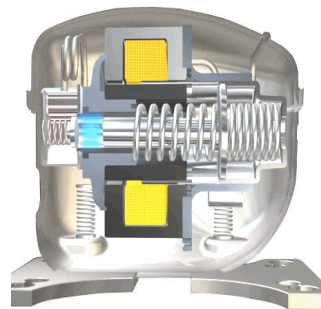


Fig. 1 Mechanical structure of a linear compressor

Since the magnetic flux density varies depending on the piston position, the force constant and the effective inductance are functions of the piston position. The effective resistance is assumed to be constant because its variance, being negligible, is ignored. is the applied voltage to the linear motor, is the current flowing through the winding coil, and is the piston position. The mechanical equation of motion can be described as:

$$M \frac{d^2x(t)}{dt^2} + C \frac{dx(t)}{dt} + Kx(t) = \alpha i(t) - A_p \Delta P(t) \tag{3}$$

where , , and denote the equivalent mass, viscous damping coefficient, and spring constant, respectively. is the cross-sectional area of the piston, is the pressure difference between the compressor chamber and the back surface of the piston. Taking the Laplace transform of the above Eqs. (1–3) yields:

$$X(s) = G(s)V(s) + W(s)\Delta P(s) \tag{4}$$

$$G(s) = \frac{\alpha}{ML_e s^3 + (MR_e + CL_e)s^2 + (CR_e + \alpha^2 + L_e K)s + R_e K} \tag{5}$$

$$W(s) = \frac{(L_e s + R_e)A_p}{ML_e s^3 + (MR_e + CL_e)s^2 + (CR_e + \alpha^2 + L_e K)s + R_e K} \tag{6}$$

A closed-loop linear compressor control system needs piston position information. In order to measure the piston position, an inductive position sensor, in which the inductor is a small stationary coil wound on a ferrite coil, can be used. However, this position sensor is more expensive than a current or voltage sensor. It is also hard to install a position sensor in a linear compressor. Hence, it is more desirable to estimate the piston position indirectly. Rearranging Eq. (1), one obtains:

$$\frac{dx(t)}{dt} = \frac{1}{\alpha} \left( V(t) - L_e \frac{di(t)}{dt} - R_e i(t) \right) \tag{7}$$

The estimated value of the piston position can be obtained by integrating Eq. (7):

$$\hat{x}(t) = \int_0^t \left(\frac{dx}{d\tau}\right) d\tau$$

$$= \frac{1}{\alpha} \int_0^t [V(\tau) - R_e i(\tau)] d\tau - \frac{L_e}{\alpha} i(t) \tag{8}$$

For a digital control system, can be modified to digital form as

$$\hat{x}(n) = \frac{T}{\alpha} \sum_{k=1}^n \left(\frac{V(k-1)+V(k)}{2}\right) - \frac{TR_e}{\alpha} \sum_{k=1}^n \left(\frac{i(k-1)+i(k)}{2}\right) - \frac{L_e}{\alpha} i(n), \quad n = 1,2,3,\dots \tag{9}$$

where  $T$  is the sampling period.

Figure:

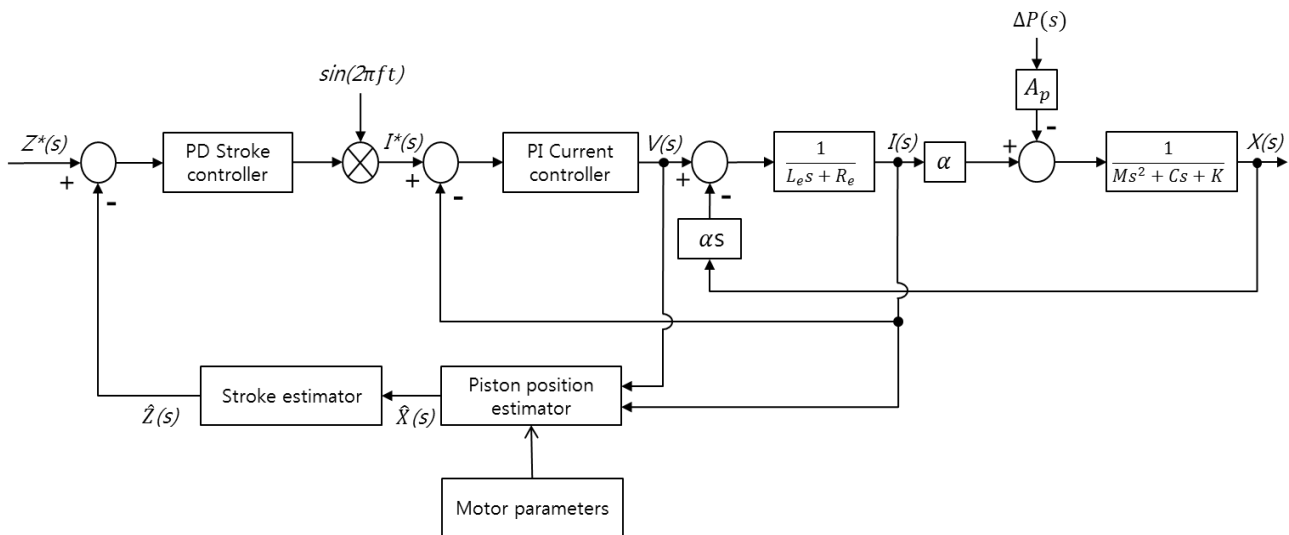


Fig. 2 Block diagram of the closed-loop sensorless stroke control system

In general, the stroke is defined as the distance between the top and bottom piston positions during one cycle of operation. Therefore, the estimated stroke can be easily calculated using the estimated piston position. Let a phase delay filter be defined as:

$$H_d(s) = \frac{2\pi f - s}{2\pi f + s} \tag{10}$$

where  $f$  is the running frequency of the piston. If  $\hat{x}_d$  is assumed to be the phase delayed output of  $\hat{x}$ , then the estimated stroke can be calculated as

$$\hat{z}(t) = \sqrt{\hat{x}^2(t) + \hat{x}_d^2(t)} \tag{11}$$

Fig. 2 shows the block diagram of the closed-loop sensorless stroke control system for a linear compressor. The applied voltage and the motor current are measured and input to the digital signal processor (DSP) central processing unit (CPU) chips after analog-to-digital (A/D) conversion. These measured variables, together with motor parameters, are used to estimate the piston position as shown in Eq. (9). The estimated stroke is compared

with the set-point value of the stroke which is determined depending on load conditions. The output of the proportional–derivative (PD) stroke controller is the set-point value of the amplitude of the motor current. The inner proportional–integral (PI) current controller is intended to minimize the effects of back EMF and current transients on the outer stroke control loop.

### III. MOTOR PARAMETER IDENTIFICATION OF LINEAR MOTOR

As mentioned earlier, the motor parameters and vary depending on the piston position. Therefore, if one assumes that the motor parameters are constant, then the estimated piston position expressed in Eq. (9) (or Eq. (8)) will have some errors, resulting in deterioration of the dynamic performance of the closed-loop sensorless stroke control system shown in Fig. 2. The motor parameters and , which have substantial influence on the dynamic performance of the closed-loop stroke control system, should be identified as functions of piston position and motor current, stored in a ROM table, and used for the accurate estimation of piston position. In general, for any operating condition of refrigerators or air conditioners, there exists an optimal stroke value for maximum efficiency. Therefore, if there are some errors in the stroke estimate, it would be difficult to achieve maximum efficiency. From Eq. (1), one obtains:

$$\hat{\alpha}x(t) + \hat{L}_e i(t) = \int_0^t [V(\tau) - R_e i(\tau)] d\tau \quad (12)$$

Note that  $\hat{\alpha}$ ,  $\hat{L}_e$ , and  $i$  in Eq. (12) are the measured values using a piston position sensor, a current sensor, and a voltage sensor, respectively. Note also that  $\alpha$  and  $L_e$  are the identified values of  $\alpha$  and  $L_e$ , respectively. Let  $T$  be a period of the piston moving linearly in the steady state. By dividing  $T$  into equal time intervals such as  $0, \dots, T$ , we obtain Eq. (13) using Eq. (12).

$$\begin{aligned} \hat{\alpha}x(t_1) + \hat{L}_e i(t_1) &= \int_0^{t_1} [V(\tau) - R_e i(\tau)] d\tau \\ \hat{\alpha}x(t_2) + \hat{L}_e i(t_2) &= \int_0^{t_2} [V(\tau) - R_e i(\tau)] d\tau \\ &\vdots \\ \hat{\alpha}x(t_n) + \hat{L}_e i(t_n) &= \int_0^{t_n} [V(\tau) - R_e i(\tau)] d\tau \end{aligned} \quad (13)$$

Rearranging Eq. (13) into matrix form, one can obtain:

$$A \begin{bmatrix} \hat{\alpha} \\ \hat{L}_e \end{bmatrix} = b \quad (14)$$

where  $n \times 2$  matrix  $A$  and  $n \times 1$  vector  $b$  are given as:

$$A = \begin{bmatrix} x(t_1) & i(t_1) \\ x(t_2) & i(t_2) \\ \vdots & \vdots \\ x(t_n) & i(t_n) \end{bmatrix}, b = \begin{bmatrix} \int_0^{t_1} [V(\tau) - R_e i(\tau)] d\tau \\ \int_0^{t_2} [V(\tau) - R_e i(\tau)] d\tau \\ \vdots \\ \int_0^{t_n} [V(\tau) - R_e i(\tau)] d\tau \end{bmatrix} \quad (15)$$

Using pseudo inverse manipulation, one can obtain Eq. (16) from Eq. (14).

$$\begin{bmatrix} \hat{\alpha} \\ \hat{L}_e \end{bmatrix} = (A^T A)^{-1} A^T b \quad (16)$$

The experimental apparatus of a sensorless stroke controller for linear compressors has been implemented as shown in Fig. 3. The CPU chip is a TMS320C2000 (Texas Instruments, USA). For experimental study, a 2.2 kW linear compressor is chosen as shown in Table 1. At first, the set-point value of the stroke is 0.02 m. The running frequency is set to 60 Hz. The identified motor parameters and obtained using Eq. (16) are shown in Figs. 4 and 5, respectively. As can be seen from Fig. 4,  $\hat{\alpha}$  is approximately 30–55 N/A for the piston position in the range of  $-0.01 \text{ m} < x < 0.01 \text{ m}$ , and the current is in the range of  $-10 \text{ A} < i < 10 \text{ A}$ . However, one can observe from Fig. 5 that  $\hat{L}_e$  is approximately 0.03–0.12 H for the same range of the piston position and the current.

Figure:

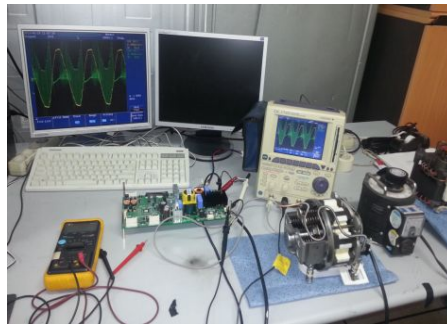


Fig. 3 Implemented experimental apparatus

Table:

Table 1. Linear motor specifications

Rated output power	2.2 kW
Rated voltage	220 V <sub>rms</sub>
Rated current	7 A <sub>rms</sub>
Rated stroke	0.02 m
Resonant frequency	60 Hz
	2.5 Ω
	55 N/A
	0.12 H

Figure:

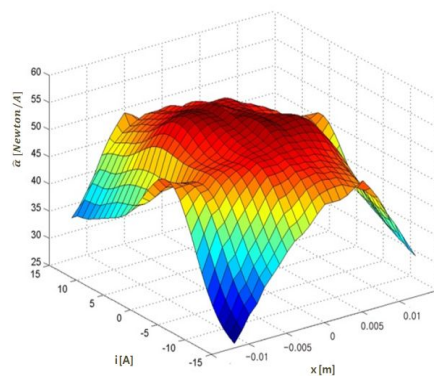


Fig. 4 Three-dimensional plot of the identified force constant .

Up to now, it has been found to be costly and difficult to install a piston position sensor for measuring the stroke. It has also been found that piston position estimation requires information of the motor parameters which are not constant and vary as functions of the piston position and the motor current. Therefore, the motor parameters and , which have substantial influence on the dynamic performance of the closed-loop stroke control system, should be identified as functions of piston position and motor current, stored in ROM table, and used for accurate estimation of piston position. However, this motor parameter identification algorithm has the demerit of demanding a large memory space for storing the identified motor parameters. Therefore, in this study, another technique is proposed for solving this problem.

Figure:

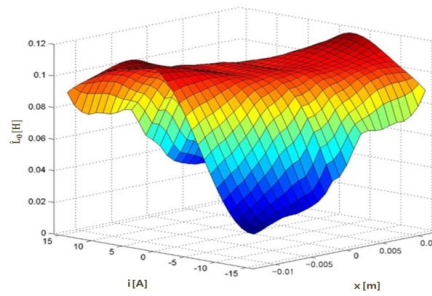


Fig. 5 Three-dimensional plot of the identified inductance

As an approach for reducing the amount of identified motor parameter data, the identified force constant shown in Fig. 4 is approximated to be the following second-order surface:

$$S(i, x, \alpha): \alpha = c_0 i^2 + c_1 x^2 + c_2 i x + c_3 i + c_4 x + c_5 \tag{17}$$

where  $i$  is the current,  $x$  is the piston position, and  $\alpha$  is the function representing the approximated force constant. Here, let  $n$  data sets of the identified force constant be  $\{(i_0, x_0, \alpha_0), (i_1, x_1, \alpha_1), \dots, (i_{n-1}, x_{n-1}, \alpha_{n-1})\}$ . Then, one obtains

$$\begin{bmatrix} \alpha_0 \\ \alpha_1 \\ \vdots \\ \alpha_{n-1} \end{bmatrix} = \begin{bmatrix} i_0^2 & x_0^2 & i_0 x_0 & i_0 & x_0 & 1 \\ i_1^2 & x_1^2 & i_1 x_1 & i_1 & x_1 & 1 \\ \vdots & \vdots & \vdots & \vdots & \vdots & \vdots \\ i_{n-1}^2 & x_{n-1}^2 & i_{n-1} x_{n-1} & i_{n-1} & x_{n-1} & 1 \end{bmatrix} \begin{bmatrix} c_0 \\ c_1 \\ c_2 \\ c_3 \\ c_4 \\ c_5 \end{bmatrix} \tag{18}$$

From this, one can obtain

$$\begin{bmatrix} c_0 \\ c_1 \\ c_2 \\ c_3 \\ c_4 \\ c_5 \end{bmatrix} = \begin{matrix} pseudo \\ inverse \\ of \end{matrix} \begin{bmatrix} i_0^2 & x_0^2 & i_0 x_0 & i_0 & x_0 & 1 \\ i_1^2 & x_1^2 & i_1 x_1 & i_1 & x_1 & 1 \\ \vdots & \vdots & \vdots & \vdots & \vdots & \vdots \\ i_{n-1}^2 & x_{n-1}^2 & i_{n-1} x_{n-1} & i_{n-1} & x_{n-1} & 1 \end{bmatrix} \begin{bmatrix} \alpha_0 \\ \alpha_1 \\ \vdots \\ \alpha_{n-1} \end{bmatrix} \tag{19}$$

Using  $n$  data sets of the identified force constant  $\hat{\alpha}$  given in Fig. 4, Eq. (19) is solved, and the second-order approximation of  $\hat{\alpha}$ , shown in Fig. 6, is finally obtained. Similarly, the identified inductance  $\hat{L}_e$  shown in Fig. 5 can also be approximated to the second-order surface:

$$S(i, x, L): L = d_0 i^2 + d_1 x^2 + d_2 i x + d_3 i + d_4 x + d_5 \tag{20}$$

Using the similar procedure as Eqs. (17–19), we can obtain  $d_i (i = 0, 1, \dots, 5)$  and the result shown in Fig. 7. Fig. 8 shows the error between Fig. 5 and Fig. 7. Next, the identified inductance  $\hat{L}_e$  shown in Fig. 5 can be approximated to the forth-order surface and sixth-order surface as shown in Fig. 9 and Fig. 10, respectively. But, in these cases, the computational time for identifying of  $L$  would be long.

Figure:

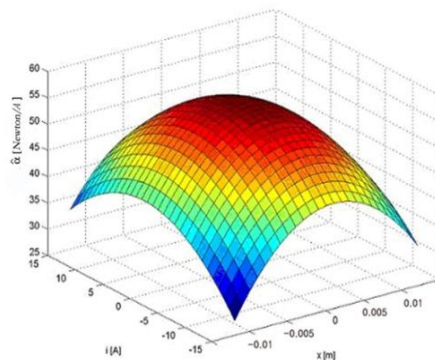
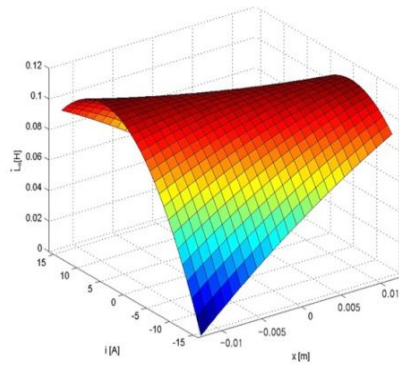


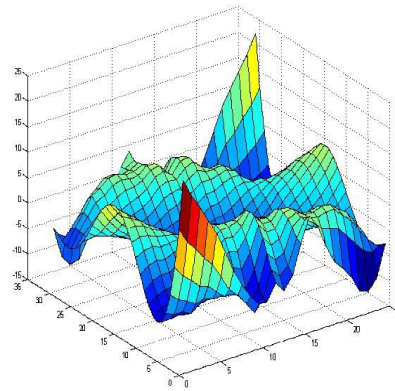
Fig. 6 Second-order approximation of

Figure:



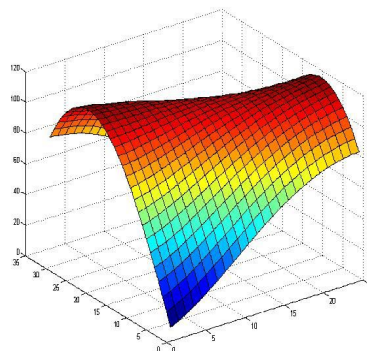
*Fig. 7 Second-order approximation of*

Figure:



*Fig. 8 Error graph*

Figure:



*Fig. 9 Forth-order approximation of*

Figure:

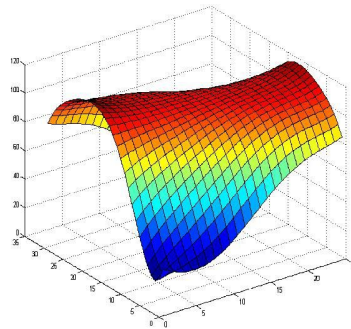


Fig. 10 Sixth-order approximation of

In order to decrease the computational time for identifying of motor parameters, we may try to do first-order approximation of motor parameters and divide the current-stroke space into several parts as Fig. 11. Fig. 12 shows the first-order approximation of obtained after operation space division is done.

Figure:

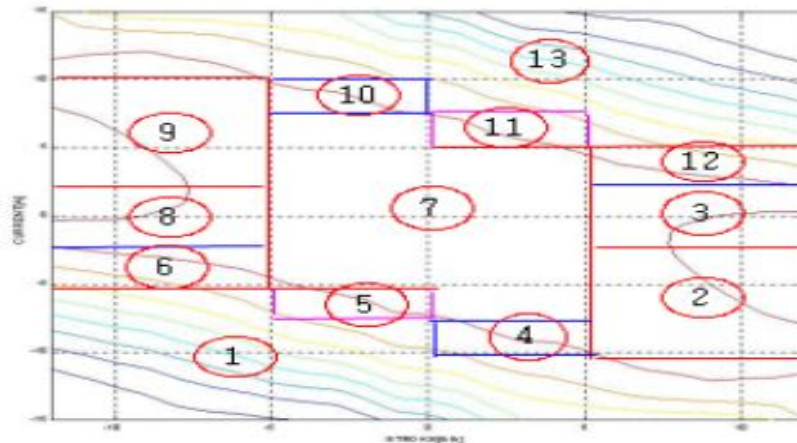


Fig. 11 Operation space divided into several parts

Figure:

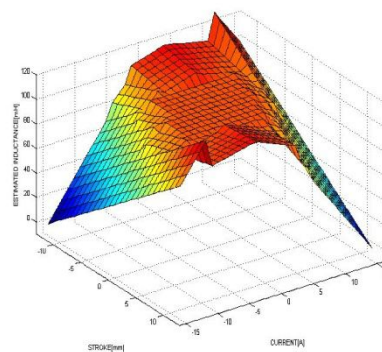


Fig. 12 First-order approximation of after operation space division

Figure:

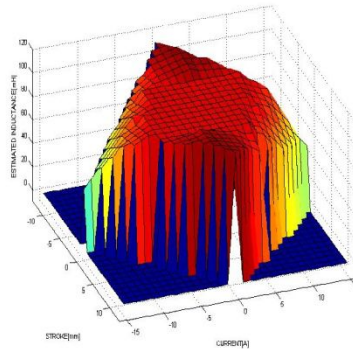


Fig. 13 First-order approximation of in case of compressor operation

Fig. 13 shows the distribution of in case of compressor real operation. Hence, even though the first-order approximation of identified motor parameters, the errors might be decreased.

#### IV. CONCLUSION

In this paper, a sensorless linear compressor control system with motor parameter identification is implemented. Various motor parameter identification algorithms are evaluated to demonstrate the practical significance of our results. Using the operation space division, we found that the errors of motor parameter identification might be decreased even though the first-order approximation of identified motor parameters was done.

#### V. ACKNOWLEDGEMENTS

This research was supported by Basic Science Research Program through the National Research Foundation of Korea(NRF) funded by the Ministry of Education, Science and Technology(No.2011-0023587)

#### REFERENCES

1. Reuven Unger, "Development and testing of a linear compressor sized for the european market," *Proceedings International Appliance Technical Conference*, pp.74–79, May, 1999.
2. Masayuki Sanada, Shigeo Morimoto, and Yoji Takeda, "Analyses for sensorless linear compressor using linear pulse motor," *Proceedings Industry Applications Conference*, pp. 2298–2304, Oct., 1999.
3. Yee-Pien Yang and Wei-Ting Chen, "Dual stroke and phase control and system identification of linear compressor of a split-stirling cryocooler," *Proceedings Decision and Control*, pp.5120–5124, Dec., 1999.
4. Gye-young Song, Hyeong-kook Lee, Jae-yoo Yoo, Jin-koo Park, and Young-ho Sung, "Development of the linear compressor for a household refrigerator," *Proceedings Appliance Manufacturer Conference & Expo*, pp.31-38, Sept., 2000.
5. Hyuk Lee, Sunghyun Ki, Sangsub Jung, and Won-hag Rhee, "The innovative green technology for refrigerators - Development of Innovative linear compressor-," *International Compressor Engineering Conference at Purdue*, pp.1419-1424, July, 2008.
6. B. J. Huang and Y. C. Chen, "System dynamics and control of a linear compressor for stroke and frequency adjustment," *Journal of Dynamic Systems, Measurement, and Control*, Vol.124, pp.176-182, March, 2002.
7. Kyeong-bae Park, Eun-pyo Hong, Ki-chul Choi, and Won-hyun, Jung, "Linear compressor without position controller," *International Compressor Engineering Conference at Purdue*, pp.C119-C125, July, 2004.
8. N. Chen, Y. J. Tang, Y. N. Wu, X. Chen, and L. Xu, "Study on static and dynamic characteristics of moving magnet linear compressors," *Cryogenics*, vol.47, pp.457–467, 2007.
9. Tae-Won Chun, Jung-Ryol Ahn, Hong-Hee Lee, Heung-Gun Kim, and Eui-Cheol Nho, "A novel strategy of efficiency control for a Linear compressor system driven by a PWM inverter," *IEEE Trans. on Industrial*

- Electronics, Vol.55, No.1, pp.296-301, Jan., 2008.*
10. Jinquan Zhang, Yunfeng Chang, and Ziwen Xing, "Study on self-sensor of linear moving magnet compressor's piston stroke," *IEEE Sensors Journal, Vol.9, No.2, pp.154-158, Feb., 2009.*
  11. Gyu-Sik Kim, "Sensorless control for linear compressors," *The Trans. of The Korean Institute of Power Electronics, Vol.10, No.5, pp.421-427, Oct., 2005.*
  12. Zhengyu Lin, Jiabin Wang, and David Howe, "A learning feedforward current controller for linear reciprocating vapor compressors," *IEEE Trans. on Industrial Electronics, Vol.58, No.8, pp.3383-3390, Aug., 2011.*